Characterization of Silane Nanoadhesion by means of Dynamic Force Spectroscopy

A. Ptak[*], M. Makowski[*], M. Niemier[*], M. Cichomski[**], H. Gojzewski[*,***] and R. Czajka[*]

[*]Institute of Physics, Poznan University of Technology, Poznan, Poland, arkadiusz.ptak@put.poznan.pl
[**]Department of Chemical Technology and Environment Protection, University of Lodz, Lodz, Poland
[***]Max Planck Institute for Polymer Research, Mainz, Germany

ABSTRACT

Using a modified atomic force microscope the nanoadhesion between a silicon tip and a monolayer of 1H, 1H, 2H, 2H-perfluorodecyl-trichlorosilane was measured at different loading rates. Adhesion force-versus-loading rate curves could be fitted with two logarithmic terms, indicating a two-energy-barrier interaction potential. The application of the Bell-Evans model to the analysis of the curves allowed extracting quantitative information about the effective adhesion potential and characterizing the different components contributing to the nanoadhesion. Although van der Waals interactions appear only major contribution to the nanoadhesion, the interaction potential characterizing the nanoadhesion has still a complex, two-barrier character.

Keywords: adhesion, AFM, Bell-Evans model, loading rate, silanes

1 INTRODUCTION

Characterization of the nanoadhesion (i.e. nanocontact adhesion) of silane compounds is of interest in various scientific disciplines and engineering for several reasons. Firstly, at the nanoscale adhesion often emerges as a dominant force. Secondly, various silane compounds have found applications in several industries from lubricants to bio-implants mostly as coupling or adhesion agents. Finally, although adhesion of macroscopic contacts has been widely studied for decades, there is no good method to recognize adhesive interactions (bonds) contributing to resultant adhesion [1].

The best tool able to probe mechanical properties of materials at the nanoscale is the atomic force microscope (AFM) [2]. To study nanoadhesion, the so-called force spectroscopy mode is used, where the interaction of an AFM tip with a sample surface is probed. The sample is mounted on a piezo translator and moved up and down while recording the deflection of the AFM cantilever due to the surface forces, resulting in a force-displacement curve.

Unfortunately, force spectroscopy does not provide complete information about the effective interaction potential determining interactions between the AFM tip and the surface of a sample [3]. If the tip-sample interaction force is attractive (usually because of van der Waals interactions) and the gradient of the force is bigger than the spring constant of the cantilever an instability occurs and the tip jumps into contact with the sample. A similar instability occurs during retracting the cantilever from the sample. At some point of the retraction trajectory the restoring force of the cantilever becomes larger than the adhesion force and the tip jumps out of contact with the sample. Therefore, an activation barrier of the adhesion forces (or several barriers in case of more complex interactions) is not sampled.

For this reason we applied the so-called dynamic force spectroscopy (DFS) that is the measurement of adhesion force versus the force loading rate (i.e. the change in pulling force per time). It is commonly observed that the adhesion force increases with the loading rate. This has been noticed independently in several disciplines with various explanations [4-6]. For instance in macroscopic adhesion it has been ascribed in most cases to energy dissipation within the bulk of the sample [4]. The most commonly used models to describe mechanical-adhesive interactions are the Johnson-Kendall-Roberts model [7], the Derjaguin-Muller-Toporov model [8], and the more general Maugis theory [9]. All these models are based on a balance between potential energy, surface energy, and elastic deformation within the solid bodies but kinetic effects are ignored in this line of analysis. Therefore we applied the Bell-Evans model [10, 11] to the nanocontact adhesion. In this case tip-sample interactions were treated as a single, effective bond although of complex nature. The objective of this paper was an application of the dynamic force spectroscopy and the Bell-Evans model for the characterization of the nanoadhesion between fluoroalkyl silanes and a silicon AFM tip .

2 THEORY

A theoretical explanation of the loading rate dependence for a single chemical bond was introduced by Evans and Ritchie [11] on the base of the Bell model [10]. The model treats the unbinding process as a kinetic problem of the escape from a potential well under the influence of the external loading force. This external load tilts the interaction potential and facilitates thermally activated escape from the bound state (see Figure 3). Then the rate constant of dissociation in the presence of loading force *F* is expressed as:

$$k_{off} = \frac{1}{\tau_D} \exp\left(-\frac{E_0 - F(t)x_\beta}{k_B T} \right), \quad (1)$$

where, E_0 is the height of the activation energy barrier, x_β is the distance between the bound state and the transition state along the direction of the external pulling force, τ_D is the characteristic diffusion time of motion in the system, k_B is the Boltzmann constant, and T the temperature. The loading force can be ramped in time:

$$F(t) = r_F t, \quad (2)$$

where r_F is the force loading rate. The solution of Eq. (1) gives the following expression for the most probable unbinding force:

$$F_{ad} = F_\beta \ln\left(\frac{r_F}{F_\beta k_{off}^0} \right), \quad (3)$$

where $F_\beta = k_B T/x_\beta$ is the so-called thermal fluctuation force [11]. Thus, F_{ad} increases linearly with $ln(r_F)$ and Eq. (3) provides a way to extract the value of x_β and the thermal dissociation constant k^0_{off} (force-free kinetic off-rate) respectively from the slope and intercept of the F_{ad} vs. $ln(r_F)$ curve fitted to experimental data. The most probable unbinding force equals a mean adhesion force for symmetrical distributions of adhesion force, what is the case of our measurements.

3 MATERIALS AND METHODS

3.1 Monolayer of fluoroalkyl silanes

Pieces of approximately 5 x 5 x 0.5 mm^3 were cut from a p-type Si(100) wafer (Cemat Silicon S.A.) and ultrasonically cleaned in anhydrous ethyl alcohol and then de-ionized water for 10 min each to minimize the surface contamination. Then the surface of the Si substrates was activated using oxygen plasma. The activated substrates were placed into a vapor phase deposition system and kept under low pressure (0.1 Pa) at 60 °C for 30 min before modification by fluoroalkyl silanes [12]. The modification of the Si substrates was performed with 1H, 1H, 2H, 2H-perfluorodecyl-trichlorosilane (FDTS; 97%, ABCR, GmbH & Co. KG Karlsruhe). The FDTS molecules chemically adsorbed onto the Si surface, forming a monolayer. The samples were stored in the modifier's vapor at room temperature for 12 h and finally outgassed under low pressure at 40 °C for 1 h in order to remove any excess of physisorbed and unreacted molecules. The samples were removed from the vacuum chamber and transferred into a vacuum desiccator until characterization.

3.2 Modified AFM system

Two major components were added to a commercial AFM (EasyScan2, Nanosurf AG, Switzerland) to extend the range of accessible loading rates: an additional z-piezo actuator (PL055.21, PI Ceramic, Germany) and a measurement/data acquisition system PXI (National Instruments, USA) containing a digital oscilloscope card NI-PXI 5122 and a waveform generator card NI-PXI 5412 (Figure 1). With these added components, the frequency of ramping the piezo up and down is limited by the mechanical properties of available AFM cantilevers [13]. The best suited cantilevers for our measurements were silicon PPP-ZEILR cantilevers (Nanosensors, Switzerland) with a nominal spring constant of 1.6 N/m and a resonance frequency of 27 kHz. With these cantilevers loading rates up to $4 \cdot 10^8$ nN·s^{-1} were achieved, which is over three orders of magnitude higher than in DFS experiments with commercial AFMs [5, 6]. To control the loading rate independently of the contact time a trapezoidal signal from the waveform generator card was applied to drive the piezo actuator. In this way we could keep the contact time constant while varying the speed of the retracting movement.

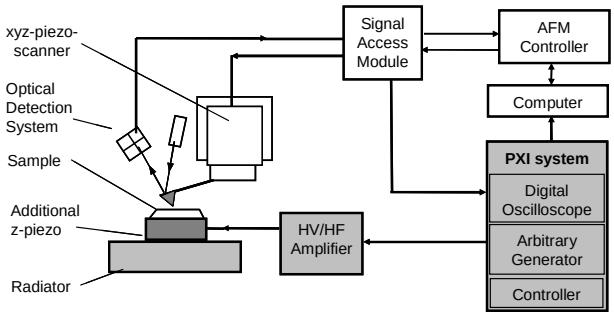

Figure 1: Schematic of the modified AFM. Gray color indicates added devices.

3.3 Dynamic Force Spectroscopy

We measured adhesion force as the average of the pull-off jumps in the retraction part of force curves. To measure adhesion force as a function of loading rate, we kept the maximal load constant at 10 nN and we varied the retraction rate. AFM typically requires knowledge of the cantilever spring constant in order to determine the force from the cantilever deflection. Spring constants were calculated from the geometry and resonant frequency of the cantilevers. To quantify the fluctuations of pull-off deflection (pull-off force) caused by the variations in the tip-sample contact area, we recorded hundreds individual pull-off forces for every loading rate. We also varied the loading rates in a random order to avoid introducing a systematic error in the data associated with tip wear and deformation of the molecular layer. The measurements were taken for various spots of two different samples.

4 RESULTS

In the range of loading rates from $7 \cdot 10^5$ to $4 \cdot 10^8$ nN s^{-1} adhesion forces increased with increasing loading rate (Figure 2). The fitting with the Bell-Evans model was performed for two loading rate regimes: 1 - from $7 \cdot 10^5$ to 10^7 nN$\cdot s^{-1}$ and 2 - from $4 \cdot 10^7$ to $4 \cdot 10^8$ nN$\cdot s^{-1}$. We omitted the transition points between the regimes. The fitting for more than two loading rate regimes does not improve significantly the fitting accuracy.

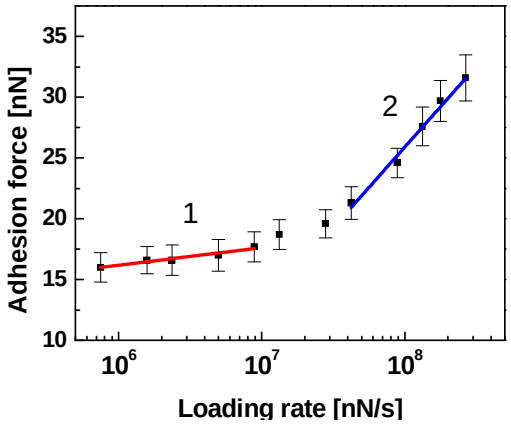

Figure 2: Adhesion force-versus-loading rate curve for nanoadhesion between a silicon tip and a monolayer of fluoroalkyl silanes. The error bars were calculated as a standard deviation of mean. The red and blue curves are fits with the Bell-Evans model for two fitting regimes: 1 – loading rates from $7 \cdot 10^5$ to 10^7 nN$\cdot s^{-1}$ and 2 – loading rates from $4 \cdot 10^7$ to $4 \cdot 10^8$ nN$\cdot s^{-1}$.

$F_{ad} = a \ln(r_f) - b$	
fitting regime 1	fitting regime 2
a = 0.6 ± 0.1 [nN]	a = 5.8 ± 0.4 [nN]
b = -7.5 ± 1.3 [nN]	b = 80 ± 8 [nN]
χ^2 = 0.02	χ^2 = 0.14

Table 1: Fitting parameters according to the Bell-Evans model. F_{ad} – the adhesion force [nN], r_f – the dimensionless loading rate [(nN$\cdot s^{-1}$)/ (nN$\cdot s^{-1}$)].

The values of the errors of calculated parameters, as well as of $\chi 2$ are relatively small (Table 1). It suggests that the Bell-Evans model, which is valid for single bonds, can be applied to nanoadhesion. This implies that the adhesive bonds within a nanocontact are not considered individually but rather lumped into one effective tip-sample interaction potential. The bi-logarithmic character of the adhesion force-versus-loading rate dependence can be interpreted by assuming that the effective interaction potential consists of two activation barriers (Figure 3). We cannot exclude the existence of more than two barriers but these two are dominant and they govern the nanoadhesion phenomenon. Barrier 1 determines the detachment at low loading rates (regime 1) and barrier 2 determines the detachment at high loading rates (regime 2). We would like to emphasize that barrier 2, which is an inner barrier, could not be detected by using a commercial AFM system because of the limited range of accessible loading rates (usually up to 10^5 nN$\cdot s^{-1}$). Each of the barriers characterizes a different kind of adhesive interactions contributing to the effective adhesion between fluoroalkyl groups of FDTS and the oxide surface of the silicon tip. We calculated kinetics and barrier parameters for both contributions (Table 2).

Barrier	Calculated parameters			
	x_β [nm]	t^0_{off} [s]	ΔE_0 [J]	ΔE_0 [k_BT]
1	$6.4 \cdot 10^{-3}$	$9.7 \cdot 10^4$	$9.6 \cdot 10^{-20}$	24
2	$7.0 \cdot 10^{-4}$	$5.2 \cdot 10^{-6}$		

Table 2: Kinetics and interaction potential parameters for the tip-sample interactions treated as an effective bond. x_β - the distance between the bound state and the transition state, k^0_{off} - the thermal dissociation constant, $t^0_{off} = 1/k^0_{off}$ - the bond lifetime, ΔE – the energy difference between the two barriers.

The distance between the bound state and the transition state (i.e. the elongation needed to rupture the bond), x_β was calculated from the slope ($a = k_BT/x_\beta$) of the dependence $F_{ad} = a \ ln(r_f) - b$, and the bond lifetime, t^0_{off} from the intercept ($b = a \ ln(ak^0_{off})$), where $k^0_{off} = 1/t^0_{off}$.

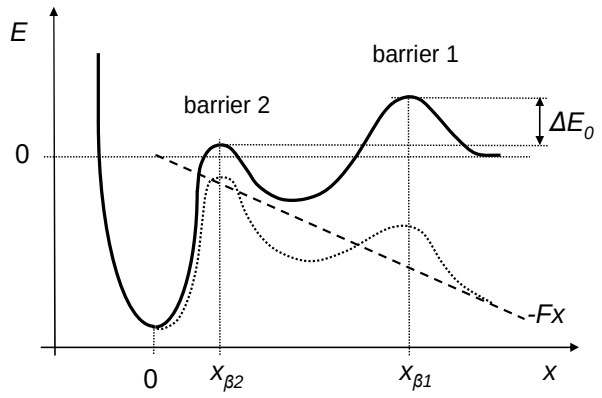

Figure 3: Conceptual interaction potential of the effective tip-sample adhesion with two energy barriers. The external force F tilts the potential and lowers the barriers. The values of x_β and ΔE_0 are in Table 2.

5 DISCUSSION AND CONCLUSIONS

On the basis of the calculated parameters of the effective tip-sample interaction potential it is possible to conclude about the interactions responsible for the nanoadhesion [14]. Barrier 1 is much higher than barrier 2 and its energy resembles that of a covalent bond. However, the extremely small value of the distance between the bound state and the transition state (0.064 Å) indicate that a number of weak bonds contribute to the nanoadhesion rather than a single, covalent bond. Performing static (at one loading rate) force spectroscopy experiments we could not conclude this. The case of barrier 2 is even more obvious because not only low energy but also very short lifetime indicate that weak interactions are related to this barrier. Capillary forces caused by condensing water are negligible because flouroalkyl silanes form a hydrophobic monolayer. Also weak chemical bonds like hydrogen bonds can be excluded from the analysis because of the chemical structure of the interacting groups. Therefore we can assume that both interaction types refer rather to van der Waals interactions.

If van der Waals interactions are only contribution to the nanoadhesion, why do they manifest in such a different way that two activation barriers are observed? The detailed answer to the question can be obtained from the analysis of the cooperativity of individual van der Waals bonds during rupture. In the case of cooperative bonds configured in parallel, the total energy barrier is a sum of individual barrier energies. The bonds act as a macro-single bond. Then, the equation for the adhesion force – loading rate dependence can be written as:

$$F_{tot} = F_\beta \ln\left(N \frac{r_F}{F_\beta k_{off}^0} \right) + \frac{(N-1)E_0}{x_\beta}, \qquad (4)$$

where N is the number of bonds [15]. There is a big rate-independent component which determines the force-rate relation and could explain the long durability of the van der Waals adhesion contribution governed by barrier 1. In the case of an uncooperative breakage of N bonds in parallel, i.e. when the bonds behave completely independently, the equation for force-rate dependence can be simplified as follows:

$$F_{tot} = NF_\beta \ln\left(\frac{r_F}{F_\beta k_{off}^0} \right) = NF_s, \qquad (5)$$

where F_s is the force distributed per one molecule [15]. If some of van der Waals bonds behave in this way, it can explain the strong force-rate dependence for the rates higher than $4 \cdot 10^7$ nN$\cdot$s^{-1}.

In conclusion, the application of the Bell-Evans model to the adhesion-versus-loading rate curves measured for the nanocontact between flouroalkyl silanes and a silicon AFM tip revealed a complex contribution of van der Waals interactions to the nanoadhesion. It demonstrates the significance of DFS experiments and particularly the extension of measurements towards higher loading rates. Measuring forces only at low loading rates as done in standard AFM experiments can miss important features of complex adhesion interactions.

Acknowledgment: A.P. thanks the Polish Ministry of Science and Higher Education for research grant No. 2859/B/H03/2008/34.

REFERENCES

[1] Allen K. W., Int. J. Adhes. Adhes. 23, 87, 2003.
[2] Binning G., Quate C. F., Gerber C., Phys. Rev. Lett. 56, 930, 1986.
[3] Butt H.-J., Cappella B., Kappl M., Surf. Sci. Rep. 59, 1, 2005.
[4] Ruths M., Granick S., Langmuir 14, 1804, 1998.
[5] Zepeda S., Yeh Y., Noy A., Langmuir 19, 1457, 2003.
[6] Maki T., Kidoaki S., Usui K., Suzuki H., Ito M., Ito F., Hayashizaki Y., Matsuda T., Langmuir 23, 2668, 2007.
[7] Johnson K. L., Kendall K., Roberts A. D., Proc. R. Soc. Lond. A. 324, 301, 1971.
[8] Derjaguin B. V., Muller V. M., Toporov Y. P. J., Colloid Interface Sci. 53, 314, 1975.
[9] Maugis D. J., Colloid Interface Sci. 150, 243, 1992.
[10] Bell G. I., Science 200, 618, 1978.
[11] Evans E., Ritchie K., Biohys. J. 72, 1541, 1997.
[12] Hozumi A., Ushiyama K., Sugimura H., Takai O., Langmuir 15(22), 7600, 1999.
[13] Ptak A., Kappl M., Butt H.-J., Appl. Phys. Lett. 88, 263109, 2006.
[14] Ptak A., Kappl M., Moreno-Flores S., Gojzewski H., Butt H.-J., Langmuir 25(1), 256, 2009.
[15] Evans E., Annu. Rev. Biophys. Biomol. Struct. 30, 105, 2001.